6-2015

Flow Cytometry and Biochemical Analysis of Apoptotic Mouse HT-2 T - Lymphocytes

Nell Pinkston
Union College - Schenectady, NY

Flow Cytometry and Biochemical Analysis of Apoptotic Mouse HT-2 T - Lymphocytes

By:

Nell Pinkston

****

UNION COLLEGE

June, 2015

ABSTRACT

PINKSTON, NELL Flow Cytometry and Biochemical Analysis of Apoptotic Mouse HT-2 T - Lymphocytes
Department of Biological Sciences, June 2015.

ADVISOR: Robert J. Lauzon, PhD.

Apoptosis is a highly organized intracellular death program in multicellular animals. In the vertebrate immune system, apoptosis plays a central role in preventing the emergence of autoreactive lymphocytes. In this study, we used multiple stimuli (staurosporine, camptothecin, and cytokine deprivation - interleukin-2 or IL-2) to initiate apoptosis in IL-2 dependent, mouse HT-2 T-lymphocytes. All three inducers triggered DNA laddering and phosphatidylserine externalization. Propidium iodide staining and flow cytometry were also used to determine whether apoptotic cells accumulated in a specific stage of the cell cycle, and whether the mode of induction affected cell cycle distribution. Our findings indicate that IL-2 deprivation induces HT-2 cells to accumulate in G1, while cells treated with staurosporine and camptothecin accumulated in G2/M and S phase, respectively. We also used immunopblotting detection to investigate $P27^{Kip1}$ protein expression for each condition. $P27^{Kip1}$ is a member of the Cip/Kip family of cyclin-dependent kinase inhibitors whose function is to enforce the G1 restriction point. We found that $P27^{Kip1}$ levels were significantly increased within 12 hrs and 6 hrs following both IL-2 deprivation and campthotecin exposure, respectively. Across all time points in the staurosporine experiments, $P27^{Kip1}$ steady state levels were decreased. These results suggest that the mode by which apoptosis is induced differentially affects cell cycle distribution.

Table of Contents

Introduction 1

Methods 8

Culturing from frozen stock 8

Cell line maintenance 8

Determining optimal cell concentration for DNA extraction from IL-2 deprived cells 9

Empirical determination of optimal cell and inducer concentrations for genomic DNA isolation from camptothecin-treated cells 9

Determining optimal cell concentration for genomic DNA isolation from staurosporine-treated cells 10

Genomic DNA isolation 10

Agarose gel electrophoresis 11

Cell cycle analysis 11

Lysate preparation 12

Protein quantification 12

SDS-PAGE and western blotting 13

Immunostaining and analysis 14

Annexin staining for early apoptosis 15

Results 16

Optimizing cell and inducer concentrations through DNA fragmentation analysis 16

Cell cycle analysis using flow cytometry 16

Annexin V staining is an early marker of apoptotic HT-2 lymphocytes: a flow cytometry analysis 17

$P27^{Kip1}$ protein levels are up-regulated in apoptotic HT-2 cells following induction with IL-2 deprivation and camptothecin 17

Discussion 19

Effectiveness of the inhibitors 19

The pre-apoptotic response 20

Early apoptotic changes and $P27^{Kip1}$ expression 22

Future work 24

Acknowledgments 26

References 27
Appendix 31
Figure 1: Electrophoresis gel DNA fragmentation after 24-hour incubation 31
Figure 2: Flow cytometry cell cycle analysis following a 36-hour time course IL-2 deprivation treatment 33
Figure 3: Flow cytometry cell cycle analysis following a 24-hour time course with 6 mM camptothecin treatment 35
Figure 4: Flow cytometry cell cycle analysis following a 24-hour time course with 1 uM staurosporine treatment 37
Figure 5: Flow cytometry analysis of Annexin V staining following a 24-hour IL-2 deprivation time course 39
Figure 6: Flow cytometry analysis of Annexin V staining following a 24-hour time course with 6 mM camptothecin 41
Figure 7: Flow cytometry analysis of Annexin V staining following a 24-hour time course with 1 uM staurosporine treatment 43
Figure 8: SDS-PAGE and immunoblotting with anti-tubulin and $P27^{Kip1}$ specific antibodies 45

Introduction

Apoptosis is a highly regulated biological process in which specific morphological and biochemical processes trigger controlled cell destruction. It is a vital contributory process to multicellular organismal development and homeostasis (Vaux, 1993). This active process is necessary for closely monitoring the disposal and recycling of contents in aged, diseased, and dying cells. Apoptosis can be characterized by three distinct phases: initiation, commitment, and execution. Initiation is marked by physiological, biological, chemical, and physical stimuli that activate the death pathway, such as phosphatidylserine externalization. The cell then undergoes physical changes, such as permeabilization of the mitochondrial outer membrane, that irreversibly commit it to death (Keeble & Gilmore, 2007). The commencement of execution is marked by phenotypic changes in the cell, including cell shrinkage, chromatin condensation, and compression of organelles without loss of ultrastructure, in the dense cytoplasm (Kerr et al., 1972). This final execution ends as the cell blebs, or pinches its contents off in small vesicles called apoptotic bodies that can be digested by neighboring or circulating phagocytes (Walsh, 2014). Highly organized and specific, this mechanism for cellular suicide removes cells with minimal accidental damage to the host organism.

Cells also undergo other, more harmful forms of cell death, the most common being necrosis. While apoptosis targets cellular destruction in individual or specific clusters of cells, necrosis distinctly affects large areas of cells (Jain et al., 2014). In contrast with apoptosis, necrotic cell death is associated with cellular swelling, loss of membrane integrity, and a severe, host inflammatory response, as necrotic cells release their contents into the surrounding tissue (Elmore, 2007). This degradative process was

once thought to be passive and energy-independent, but recent studies suggest that it may be more regulated than initially thought (Bell et al., 2008; Ch'en et al., 2008; Bell & Walsh, 2009). Similarly to apoptosis, the process is preceded by mitochondrial permeability transition: this is a genetically driven process where pores in the mitochondrial outer membrane open, disrupting salt and proton gradients and irreversibly inhibiting the organelle's function (Kroemer, 2014). Both cell death pathways can occur simultaneously, and they require close monitoring to maintain health and viability in multicellular organisms. Specifically, apoptotic deregulation can lead to terminal conditions, such as cancers, autoimmune diseases, metabolic disorders, neurogenerative diseases, and stroke (Hanahan & Weinberg, 2000; Prasad & Prabhakar, 2003; McKenzie et al., 2004; Rohn et al., 2001; Prunell et al., 2005). It is therefore important to understand this mechanism for programmed cell death, as it holds a vast array of applications in the scientific and medical fields.

Because apoptosis essentially avoids tissue inflammation, it plays an essential role in the resolution of the immune response at the organismal level (Kurosaka et al., 2003). More than simply a non-inflammatory reaction, apoptosis has been linked to promoting immunosuppressive effects of phagocytes during cell clearance (Savill & Fadok, 2000; Albert et al. 1998). The activity of phagocytes that bind and ingest apoptotic cells is a critical homeostatic mechanism that controls effector lymphocyte populations (Savill et al., 2002). Regulation of these effector immune cells have shown that apoptosis inhibits inflammation by simultaneously increasing secretion of anti-inflammatory and immunoregulatory cytokines and decreasing secretion of the pro-inflammatory cytokines (Voll et al. 1997). Lymphocytes are fast replicating, non-cancerous, and karotypically

normal cells that can regulate immune response through apoptosis. Because of their indispensable role multicellular organismal immunity, these cells are the focus of our research. The current study sought to evaluate apoptosis induction in cultured HT-2 mouse T-lymphocytes by investigating the effectiveness of various known apoptosis triggering agents.

Stimulation of apoptosis in mammalian cells can occur both intra- and extracellularly. The intrinsic pathway propagates via non-receptor mediated intracellular signals, specifically through mitochondrial release of pro-apoptotic members of the Bcl-2 protein family into the cytoplasm (Schleich & Lavrik, 2013). This pathway is often selected when a cell's DNA content is damaged or has been exposed to toxins or radiation. The extrinsic pathway requires extrinsic ligands to bind trans-membrane death receptors on the cell's membrane surface. These signaling molecules transduce the death signal to intracellular caspases that initiate the apoptotic response. Surface expression of the death receptors can vary significantly between cell types. Specifically, these receptors are often down-regulated or absent in drug-resistant cancer cell lines (Fulda, 2006). In this study, we used three known apoptosis inducers to examine both pathways.

Interleukin (IL)-2 deprivation, camptothecin, and staurosporine treatments were used to initiate the apoptotic response. IL-2 is a cytokine that binds cell surface receptors that transduce this signal via protein kinases, which in turn, are responsible for T-cell growth and survival. It is the quintessential growth factor involved in the production of T-lymphocytes (Huleatt et al., 2003). Cells incubated with this growth factor enter the cell cycle and divide. Without this growth and regulatory signaling molecule, the cell ceases to proliferate and an extrinsic apoptotic response is initiated (Tsai et al., 2013).

Camptothecin also sets off an extrinsic, death-receptor pathway, and does so by inhibiting DNA topoisomerase I (Jacobs et al., 2007). When DNA is replicated, the strands can become tightly coiled. DNA topoisomerase I functions to alleviate supercoiled DNA by clipping one of the strands, unwinding it, and rejoining the ends. Camptothecin deactivates the enzyme by binding an intermediate involved in DNA unwinding, subsequently increasing DNA cleavage without repair (Hertzberg, 1989). Initially isolated from the bark of a Chinese tree, *Camptotheca acuminata*, camptothecin was used in clinical testing in the 1970s for cancer treatment (Pommier, 2006). The drug was suspended due to associated side effects, but subsequent derivatives have continued to treat a variety of cancers, causing these cells to shrink and die (Kyle et al., 2014; Zeng et al. 2014). The final inducer used was staurosporine, an initiator of intrinsic-pathway apoptosis through kinase c inhibition (Li et al., 2009). It is known be nearly universal in its ability to induce apoptosis in nucleated cells (Bertrand et al., 1994). Staurosporine typically induces the mitochondrion-dependent pathway of apoptosis; however, provided the cell is able activate specific caspases, the pathway divides again between caspase-dependent and independent mechanisms (Castro et al., 2010; Belmokhtar et al., 2001). Given their known mechanisms for induction, the three treatments were used to disrupt normal cell division at various stages of the cell cycle. We hypothesized that IL-2 deprivation would target the G1 phase, camptothecin, S phase, and staurosporine, G2/M phase.

The initial intention of the study was to determine if the three known inducing agents also provoke changes in cell cycle distribution using flow cytometry. We also sought to correlate any of these observed changes in distribution prior to cell death with

early markers for apoptosis using annexin V staining to detect and quantify phosphatidylserine externalization via flow cytometry. We finally wished to characterize expression of critical regulatory proteins of the cell cycle. We hoped to connect their regulation and steady state levels with the time points that marked distribution changes and early apoptotic changes.

$P27^{Kip1}$ is a G1/S phase cyclin-dependent kinase (cdk) inhibitor that stops cells at the G1/S phase boundary (Levkau et al., 1998). Movement of cells from G1 into S phase is regulated specifically by cdk2, a cyclin-dependent kinase enzyme that forms a complex with cyclin A and E, and facilitates progression through the cell cycle. Cell cycle arrest at the G1/S phase boundary by $P27^{Kip1}$ has been found to cause apoptosis in both cancerous and non-cancerous cell lines, including mesangial cells, fibroblasts, endothelial cells, small cell lung cancers, erythroleukemia cells, and T-lymphocytes (Hiromura et al., 1999; Lavkau et al., 1998; Masuda et al., 2001; Drexler & Pebler, 2003; Huleatt et al., 2003). While the significance of this G1/S phase check point and importance of $P27^{Kip1}$ is agreed upon in the field, debate over how exactly $P27^{Kip1}$ regulates apoptotic pathways continues.

Excess levels of the protein have been found to both promote and discourage entrance of cells into apoptosis. Some studies suggest that $P27^{Kip1}$ inhibitor can serve to protect cells from apoptosis by constraining cdk2 activity (Hiromura et al., 1999). In the absence of specific growth factors, CDK2 activity leads to apoptosis. Further studies attribute cell enhanced survival rate to proteasome inhibitor protection caused by the expression of $p27^{Kip1}$ (Drexler & Pebler, 2003). Other investigators have found that upregulation of $p27^{Kip1}$ levels protect cells from apoptosis in unfavorable

microenvironments, such as hypoxic or low nutrient conditions (Masuda et al., 2001). In contrast, other studies have uncovered that cell proliferation and differentiation require low levels of $P27^{Kip1}$ (Hiromura et al., 1999). Steady state levels of the cdk inhibitor may not be the sole determining factor of cellular demise, but rather work in conjunction with environmental or molecular factors. In contrast to the upregulation of $p27^{Kip1}$ in cells that were grown in low nutrient conditions, cells grown in complete medium had very few apoptotic cells (Masuda et al., 2001). While high levels of $p27^{Kip1}$ may delay the cell from transitioning to S-phase, reducing its concentration will not guarantee proliferation if cdk2 activity is compromised and all necessary growth factors are not present (Bruggeman et al., 2010). It is clear that $P27^{Kip1}$ plays an essential role in monitoring the fate of cells as they progress through the cell cycle, however the inhibitor's interplay with surrounding growth factors, environmental conditions, and enzyme interaction is not yet fully understood.

It is important to recognize that $p27^{Kip1}$'s role in proliferation is not dichotomous with its participation in apoptosis. In some instances, its upreguation has been found to retard proliferation, but not necessarily induce apoptosis (Drexler & Pebler, 2003). This characteristic is important when developing cancer treatments or connecting protein steady state levels to gene expression. Therapy for non-small cell lung cancers has been specialized to target $p27^{Kip1}$ to inhibit growth by reducing viability (Eymin & Brambilla, 2004). Other cancers respond better with reintroduced $p27^{Kip1}$ that induces apoptosis. More than simply regulating this protein's steady state levels, it is important to recognize the critical role that gene expression, post-translational modification, and intracellular localization play in the inhibitory function of $p27^{Kip1}$ in the cell. Ishii et al. (2004) studied

$P27^{Kip1}$ in human lung adenocarcinoma, and found that the extent of phosphorylation effected localization of the inhibitory protein in the cell. More complete phosphorylation status lead to greater localization to the cytoplasm, where the protein is functional. This specific localization pattern was associated with the cytoprotective function of $P27^{Kip1}$. Cytoplasmic localization of $P27^{Kip1}$ has also been associated with an anti- apoptotic function in breast cancer cells, leading to poor prognosis in these afflicted patients (Lian et al., 2002). Elucidating the many pathways involved in $P27^{Kip1}$ function and regulation may provide the answer to cell survival and fate.

The aim of this study was to further examine the role of three inducers (interleukin-2 deprivation, camptothecin and staurosporine) in initiating apoptosis and how each affected cell cycle distribution in IL-2 dependent, mouse HT-2, T-lymphocytes via flow cytometry. We hypothesized that interleukin-2 deprived cells would accumulate in G1 prior to initiating DNA fragmentation, whereas camptothecin and staurosporine exposure would induce S and G2/M phase arrest, respectively. The timeframe required for complete cellular fragmentation was also determined with each apoptosis inducer. Our findings indicate that apoptosis in IL-2 deprived and camptothecin treated cells correlated temporally with an early increase in $P27^{Kip1}$ steady state levels, and decreased expression following staurosporine treatment. Collectively, these results suggest an important interplay between the inducer's role and the cell's response to life or death in cultured mouse T-lymphocytes.

Methods

Culturing from frozen stock

HT-2 cell stocks were thawed quickly from storage in a -80^{o}C liquid nitrogen container and rested for 10 minutes at room temperature. These cells were then transferred into a sterile 15mL centrifuge tube. 10mL of growth medium made with Dulbecco's Modified Eagle's Medium (containing 5 mM D-glucose), 5 x 10^{-5} M beta-mercaptoethanol, 2m M L-glutamine, 50 μg/mL gentamycin, 10 mM Hepes buffer pH = 7.2, 10% interleukin-2 (Roche, Indianapolis, IN), and 10% fetal bovine serum (Atlanta Biologicals, Flowery Branch, GA) was added slowly to the cells over 5 minutes. The cell/media mixture was then centrifuged at 8000rpms, 12^{o}C for 8 minutes, decanted, and resuspended in 10 mL of growth media. The cells were transferred to a culture flask (Sigma-Adlrich, St. Louis, MS) and incubated at 5% CO_2 at 37^{o}C.

Cell line maintenance

The cells were maintained at the indicated cell concentrations shown in Table 1.

Table 1. Cell concentration maintenance.

Media Volume (mL)	10	20	30	40
Maximum Number of Cells (million cells)	4	8	12	16

Cells were passaged every 4-5 days and seeded at a density of 10^4 cells/mL.

Determining optimal cell concentration for DNA extraction from IL-2 deprived cells

HT-2 cells were grown to a density of 8 million in a final volume of 20 mL IL-2 (+) medium, transferred to two 15 mL tubes, and centrifuged at 1200 rpms, 12^{o}C for 8 minutes. The cells were washed twice in 10 mL IL-2 (–) media and seeded into four, 10 mL flasks. Two flasks containing 10 mL IL-2 (+) media served as controls and grown to a density of 200,000 and 100,000 cells/mL, respectively. Since the cells would undergo two cell cycles in 24hr incubation period (each cell cycle was previously determined to be approximately 12 hours), one control flask was seeded with 250,000 and the other with 500,000 cells to obtain the target concentrations. The remaining two flasks contained 10 mL of IL-2 (–) media, and the cells were grown to the same density. Their volumes were selected assuming that these cells would finish their current cycle before arresting, and so one was seeded with 500,000 cells, and the other, 1,000,000 cells. Cells were grown in a humidified incubator at 37^{o}C and 5% carbon dioxide.

Empirical determination of optimal cell and inducer concentrations for genomic DNA isolation from camptothecin-treated cells

Preparation for the campthothecin experiment was similar to IL-2 deprivation, however HT-2 cells were not washed, but instead, maintained in IL-2 (+) media. Cells were incubated at 24hrs and grown to 200,000 cells/mL in all flasks. IL2 controls were prepared as described above, but experimental flasks were seeded at their final cell concentration, 200,000 cells/mL, assuming immediate arrest following toxin exposure. 30 and 60 μL volumes (6 and 12 μM respectively) of a camptothecin stock previously

dissolved in dimethysulfoxide (DMSO) and DMSO alone were added to each of the two experimental flasks and control flasks, respectively.

Determining optimal cell concentration for genomic DNA isolation from staurosporine-treated cells

Preparation for the staurosporine experiment was identical to camptothecin, except for the following: a) concentration was varied between 100,000 and 200,000 cells/mL b) 5 µL (1µM) stock staurosporine was added to each experimental c) 5 µL DMSO was added to each control d) cells were incubated for 12 hrs. Low concentrations of staurosporine had previously been observed by us and others to induce cell cycle arrest (Zong, 1999, Lauzon, unpublished observations). Because of its high potency to induce apoptosis at 1µM concentration, the incubation period for this experiment was shortened and concentration fixed to determine optimal cell concentration.

Genomic DNA isolation

Genomic DNA was isolated according to the manufacturer's specifications (Roche). Briefly, cells were transferred from their flasks to 15 mL tubes and centrifuged at 8000 rpm, 12^{o}C for 8 minutes. They were then washed in phosphate buffered saline (PBS) pH=7.4 and transferred into microfuge tubes. The cells were spun at 3000 rpms for 1 min and the cell pellet resuspended with 200 µL of PBS and 200 µL of lysis buffer. The solution was incubated at 72^{o}C for 10 minutes. After incubation, 100 µL isopropanol was added, and the lysate was transferred to a filter tube. The contents were spun through the filter tube at 8000 rpms for 1 minute and the flow-through, discarded. The cells were

washed twice in 500 µL wash buffer and spun at 8000 rpms/1min. An additional spin was carried out at 13,000 rpms for 30 seconds to remove any excess wash buffer. The filter tube was finally transferred to a clean microfuge tube and genomic DNA was eluted with 40 µL of pre-warmed elution buffer.

Agarose gel electrophoresis

Genomic DNA was size-fractionated via agarose gel electrophoresis in 50 mM Tris Acetate EDTA (TAE) buffer solution (pH = 8.0) for 60 minutes at 70 volts. DNA samples were prepared using 8 µL of isolated DNA and 2 µL EZ-vision loading dye (Amresco, Solon, OH) and electrophoresed in 2% agarose gels. Digital images were obtained using a G box gel documentation system (Syngene, Frederick, MD).

Cell cycle analysis

Given the results obtained from gel electrophoresis testing, cells were grown to 200,000 cells/mL concentrations in 10 mL flasks for all inducer experiments. Time course experiments were developed based on previous experiments, literature, and inducer behavior. IL-2 deprived cells were harvested at 12, 24, and 36 hours, and camptothecin and staurosporine at 3, 6, 12, and 24 hours. These cells were prepared for flow cytometry cell cycle analysis according to the Guava® Cell Cycle Reagent protocol (EMD Millipore, Billerica, MA).

Prior to adding the reagent, the cells were fixed in 70% ethanol. At their respective time points, incubated cells were spun at 450 x g for 5 minutes in 50 mL centrifuge tubes. Once the supernatant was removed, 25 mL of 1x PBS was added to the

tube. The cells were spun under the same conditions, and the supernatant was again removed leaving approximately 500µL in the tube. Cells were resuspended and added dropwise to a 50 mL tube containing 30 mL of ice-cold 70% ethanol while vortexing at medium speed. They were stored at 4^{o}C until flow cytometry analysis.

The alcohol-fixed cells were isolated by centrifugation and washed in 1 mL PBS. They were then transferred to a 15 mL centrifuge tube and the cell concentration was adjusted to 200,000 cells/sample. They were spun at 450 x g for 5 minutes, and the PBS supernatant was removed. 200 µL of Guava Cycle Reagent (EMD Millipore) was added to the cells. The samples were incubated for 30 minutes at room temperature in the dark prior to acquiring the data on a guava Flow Cytometry easyCyte System (EMD Millipore).

Lysate preparation

5 million HT-2 cells were incubated with 400 µl of hot lysis buffer (125 mM Tris-HCl, pH = 6.8, 2%SDS, 5% glycerol, 0.003% bromophenol blue, 1% β-mercaptethanol previously heated for three minutes at 100°C). Genomic DNA was sheared using a 26-gauge needle and syringe, and lysates were aliquoted and stored at -70°C until needed for protein quantification and sodium dodecyl sulfate polyacrylamide gel electrophoresis (SDS-PAGE).

Protein quantification

HT-2 T lymphocyte lysates were diluted 1/25 in ultrapure water. Protein standards were prepared using Bovine Serum Albumin (Thermo Scientific, Waltham, MA) in a

series of concentrations of 0 0.1, 0.2, 0.4, and 0.6 mg/mL in 4% lysis buffer previously mixed with ultrapure water. 50 μL of each lysate or BSA protein standard was mixed with 1.5 mL of Coomassie Plus Protein Assay Reagent (Thermo Scientific) and added to plastic cuvettes. Absorbances were determined using a Genesys 20 spectrophotometer (Thermo Spectronic, Waltham, MA) at 595 nm. Unknown concentrations were determined using regression analysis in Microsoft Excel.

SDS-PAGE and western blotting

20 μg of HT-2 cell lysates were used for SDS-PAGE. The lysates and 10 μl of Kaleidoscope pre-stained molecular weight standards (Bio-Rad, Hercules, CA) were boiled for three minutes at 95°C in a block heater. Samples were briefly centrifuged, placed on ice and subsequently loaded into a 4-15% Tris-HCl precast, gradient gel (Bio-Rad) placed in a mini-protean II electrophoresis apparatus (Bio-Rad). Duplicate sets of each sample were size-fractionated in 1x running buffer (5 mM Tris, 192 mM glycine, 0.1% SDS) along with 10 μl of Kaleidoscope protein standards at 120V for approximately 50 minutes or until the tracking dye reached the bottom of the gel.

The gel and a piece of Optitran Nitrocellulose membrane (Schleicher & Schuell, Keene, NH) pre-cut to the gel's dimensions were soaked for 20 minutes in transfer buffer (50 mM Tris Base, 384 mM glycine, 20% methanol, 0.01% SDS). Four pieces of Whatman filter gel blot paper (Schleicher & Schuell) cut to the same dimensions as the membrane and gel were also soaked for 20 minutes in transfer buffer, and the gel was placed atop two pieces of filter paper. The nitrocellulose paper was placed over the gel, and the remaining pieces of filter paper were placed on top of the membrane. The gel-

nitrocellulose sandwich was placed face down on a WD Trans-Blot apparatus (Bio-Rad) and blotted for 20 minutes at 15 volts. The nitrocellulose membrane was removed, allowed to dry and cut to size.

Immunostaining and analysis

The two membranes were placed in separate Nalgene wash containers (Thermo Scientific) for 60 minutes on a bench top circular shaker containing 10 mL of blocking buffer (5% non-fat dry milk, 10 mM Tris-HCl ph=7.5, 100 mM NaCl, 0.1% Tween 20). Blocking buffer was removed and replaced with primary antibodies in 10 mL of blocking buffer. The membrane was incubated with either a mouse monoclonal anti-alpha tubulin antibody (Sigma-Aldrich) or a rabbit polyclonal anti Kip 1 (p27) antibody (Cell Signaling Technology, Danvers, MA) at dilutions of 1:10,000 and 1:1000, respectively. Incubations with the primary antibody were carried out overnight at 4^{o}C on an orbital shaker at low speed. The nitrocellulose membrane was washed four times, ten-minutes each in wash buffer (10 mM Tris pH=7.5, 100 mM NaCl, 0.1% Tween 20). Tubulin samples were subsequently incubated with a secondary, alkaline phosphatase conjugated goat anti-mouse IgG antibody (Jackson Immunoresearch, Bar Harbor, ME), while Kip 1 (p27) samples were incubated with secondary, alkaline phosphatase conjugated goat anti-rabbit IgG antibody (Jackson Immunoresearch). Both secondary antibodies were diluted 1:1000 in blocking buffer. Incubations were carried out at room temperature on a circular shaker for 2 hours. The membranes were washed four times for ten minutes each with wash buffer and briefly rinsed in 10 mM tris/HCl buffer pH = 7.2 or ultrapure water to remove excess Tween 20 detergent. They were subsequently incubated in the dark with

200 μl of nitro blue tetrazolium/ bromo chloro indolyl phosphate (NBT/BCIP) substrate (Roche Diagnostics, Indianapolis, IN) in 10 mL of alkaline phosphatase buffer (100 mM NaCl, 5 mM $MgCl_2$, 100 mM Tris, pH=9.5) on a shaker, until color developed.

Annexin staining for early apoptosis

HT-2 cells were grown to a concentration of 200,000 cells/mL, and harvested at 12 and 24 hours for IL-2 deprivation and 3, 6, 12, and 24 hours for camptothecin and staurosporine experiments, respectively. The cells were subsequently prepared for flow cytometry analysis using the Guava® Nexin Reagent protocol (EMD Millipore). Cells were spun and resuspended in PBS with 1% fetal bovine serum (FBS) (Atlanta Biologicals). Their concentration was maintained at 200,000 cells/mL and 100μL was added to an equal volume Guava Nexin Reagent (EMD Millipore). Samples were incubated for 20 minutes at room temperature in the dark prior to acquiring the data on a guava Flow Cytometry easyCyte System (EMD Millipore).

Results

Optimizing cell and inducer concentrations through DNA fragmentation analysis

Initial testing of IL-2 deprivation, camptothecin, and staurosporine treatments identified the ideal cell and inducer concentrations required to standardize subsequent experiments. Using agarose gel electrophoresis data, internucleosomal DNA fragmentation (DNA laddering) was observed in IL-2 deprived cells at both cell concentrations, 100,000 and 200,000 cells/mL (Fig. 1a). Greater intensity of DNA laddering was observed at the higher concentration. The data showed similar intensity differences between the two cell concentrations in both the camptothecin and staurosporine experiments (Fig. 1b & 1c). Both camptothecin concentrations (6 and 12 mM) induced DNA laddering at 24 hours post-induction (Fig. 1b). To prevent concentration-induced necrosis, the lower camptothecin concentration (6 mM) was deemed sufficient for future experiments.

Cell cycle using flow cytometry

Accumulation of cells at various stages of the cell cycle was observed following the three treatments. Control HT2 cells maintained in interleukin 2 (IL-2) followed standard distribution pattern in all experiments (Fig. 2, 3, & 4 controls). IL-2 deprivation treatments characterized accumulation of cells in the G1 phase of the cell cycle (G1 DNA content) following 12 hours of withdrawal. Late stage apoptosis was observed in these cells after 24 hours, as depicted by the accumulation of cells with sub-G1 DNA content. Massive cell death followed at 36 hours of deprivation (Fig. 2). Cell behavior following camptothecin exposure was characterized by initial accumulation in the G1 phase of the

cell cycle at 3 hours post-induction that lead to later arrest in S-phase at 6 hours (Fig. 3). Apoptosis ensued at 12 hours as depicted by the accumulation of cells with sub-G1 DNA content, and all cells were dead at 24 hours. Staurosporine treatment caused cell accumulation in S- and G2/M-stage at 3 hours post-induction, later shifting to the G2/M-phase after 6 hours of exposure (Fig. 4). Significant accumulation in G2/M was visible at 12 hours, and most cells were dead at 24 hours.

Annexin V staining is an early marker of apoptotic HT-2 T lymphocytes: a flow cytometry analysis.

Early stage apoptosis marked by phosphatidylserine (PS) externalization and annexin V was observed with all three apoptosis inducers. In IL-2 deprived cells, annexin V staining was observed prior to cell membrane permeabilization (determined by staining with the fluorescent DNA binding dye 7-aminoactinomycin D or 7-AAD) between 12 and 24 hours of incubation (Fig. 5). In contrast, PS externalization was observed at 3 hours following camptothecin exposure (Fig. 6). The majority of the HT-2 cells were found to enter late stages of apoptosis by 12 hours. Staurosporine treatment consistently induced PS externalization between 6 and 12 hours post-induction, and entered late-stage apoptosis by 24 hours (Fig. 7).

$P27^{Kip1}$ protein levels are up-regulated in apoptotic HT-2 cells following induction with IL-2 deprivation and camptothecin.

Alpha-tubulin steady state protein levels were used as a housekeeping control. High levels of tubulin expression were observed across all time points and inducers (Fig.

8a, b, c). These experiments confirmed proper quantification (20 micrograms per lane) and loading of protein lysates on SDS-PAGE. $P27^{Kip1}$ steady state, protein levels increased within 12 hours of IL-2 withdrawal (Fig. 8d), and after 6 hours of camptothecin exposure relative to control samples (Fig. 8e). No significant changes in Kip1 expression were observed following staurosporine treatment, except at 24 hours, in which protein levels were downregulated (Fig. 8f).

Discussion

This research intended to better understand the role of three specific inducers in triggering apoptosis in normal, interleukin-2 dependent mouse HT-2 T-lymphocytes. Each treatment drove the cells to the same apoptotic fate, yet each led them there through very distinct pathways and different kinetics. The unique nature of each pathway is evidenced by cell cycle distribution and timing of early apoptotic markers. Each inducer provoked accumulation of cells in distinct phases of the cell cycle prior to the externalization of phosphatidylserine on their membrane surface, and subsequent DNA fragmentation and death. Further differences between the modes of apoptosis were observed through $P27^{Kip1}$ protein quantification. This critical G1/S phase checkpoint inhibitor protein was found to be significantly up-regulated in two of the treatments, IL-2 deprivation and camptothecin exposure, but down-regulated in the third (staurosporine). These data suggest that the type of inducer may also be fundamental to the role of $P27^{Kip1}$ role in either promoting or protecting from apoptosis.

Effectiveness of the inhibitors

IL-2 deprivation, camptothecin exposure, and staurosporine treatment are well known inducers of programmed cell death (Crispin et al., 2011; Zeng et al., 2012; Simenc & Lipnik-Stangeli, 2012). The current research has confirmed that each treatment is equally effective in triggering internucleosomal DNA fragmentation (DNA laddering) in HT-2 mouse T - lymphocytes. Agarose gel electrophoresis revealed that DNA laddering was visible at both camptothecin concentrations following 24 hours, and the lower of the dosage was selected for subsequent experiments to avoid necrosis. High concentrations of

apoptosis inducers, such as camptothecin or staurosporine, used to treat some cancer cell lines have been found to induce necrosis instead of apoptosis (Zare-Mirakabadi et al., 2012; Simenc & Lipnik-Stangeli, 2012). Any differences noted in band intensity here were likely due to inconsistent cell concentrations. These experiments were carried out to ensure that apoptosis was indeed stimulated by the chosen treatments. In this study, we did not carry out a time course to determine the earliest onset of DNA laddering, but it is well documented that this feature is a late event in the apoptotic pathway (Elmore, 2007).

The pre-apoptotic response

Our findings indicate that disruption of the cell cycle of HT-2 mouse T-lymphocytes is a precursor to apoptotic cell death. The cell cycle is a highly regulated process equipped with various checkpoints that assess the condition of the cell as it is replicated. Essential regulatory molecules at these checkpoints function to identify problems or errors in cell cycle progression. Depending on the severity of the defect, the cell's progression will either be stalled as repairs are performed or redirected to programmed cell death pathways. The immediacy of the transition to cell death, such as apoptosis, is debated. Some forms of apoptosis have found no effect on cell cycle distribution, indicated by immediate transition of the damaged cell out of the cell cycle and no accumulation in any particular phase (Ishii et al., 2004). Others have studied apoptosis inducers that promote alterations in cell cycle distribution, as cells accumulate at a checkpoint prior to their death (Mercier et al., 2013; Fan et al., 2014). The present study did find an effect on cell cycle distribution from the three inducers used. Induction of apoptosis resulting from IL-2 deprivation led to accumulation in the G1 phase of the

cell cycle, whereas camptothecin or staurosporine induction resulted in S and G2/M phase accumulation, respectively.

The accumulation of cells in a specific phase of the cell cycle is typically referred to as "cell cycle arrest," and this process has typically been analyzed by flow cytometry (Tong et al., 2014). There are two principal and distinct forms of cellular arrest, quiescence and senescence. Quiescence is a reversible form of cell cycle arrest usually caused by the withdrawal of growth factors or nutrients (Blagosklonny, 2011). In contrast, during senescence, the cell cycle becomes blocked by DNA damaging agents, radiation, tumor suppressors or cyclin-dependent kinase (CDK) inhibitors. However, no signals are sent to discontinue the growth-promoting pathways. This propagated growth signal results in an accumulation of cells in a given phase as the growth signals propagate. The treatments used in this study showed senescent behavior prior to entrance into apoptosis and cell fragmentation.

Evidence that implied a senescence-type response existed prior to apoptosis was first observed through cell cycle analysis, and later confirmed with annexin V staining. IL-2 deprived cells began accumulating significantly following 12 hours of incubation in IL-2-deprived media. At that time, minimal genomic DNA fragmentation was noted (i.e.: absence of cells with sub-G1 DNA content), indicating that cells were not entering late stage apoptosis as they were beginning to accumulate in G1. Detection for early stage apoptosis also indicated no apoptotic activity until cells had been deprived of IL-2 for 24 hours. Cellular arrest following camptothecin exposure occurred after 6 hours, overlapping slightly with apoptotic changes that began at 6 hours and more significantly,

at 12 hours. Finally, staurosporine experimental cells accumulated after 6 hours in G2/M phase prior to entering apoptosis at 12 hours.

Early apoptotic changes and P27^{Kip1} expression

P27^{Kip1} is a well-known inhibitor of the cyclin dependent kinase complex cdk2-cyclin A/E, and it plays an important role in regulating G1/S cell cycle arrest (Levkau et al., 1998). In the current study, P27^{Kip1} protein steady state levels increased within 12 hours following IL-2 deprivation. This increase in inhibitor concentration occurred simultaneously with phosphatidylserine externalization (annexin staining) in the induced HT-2 cells. Previous studies have shown that IL-2 withdrawal in T-lymphocytes results in G1 cell cycle arrest and upregulation of the P27^{Kip1} inhibitor (Huleatt et al., 2003). More so, Huleatt et al. found highest P27^{Kip1} levels were associated with activated (rather than deactivated) T-cells undergoing apoptosis resulting from cytokine withdrawal. These data are consistent with the behaviors of the mouse HT-2 cells. Their time course for induction however, does not coincide with that determined by the current study, as they report accumulation as early as 4 hours, and increased P27^{Kip1} steady state levels after 6 hours of incubation. Interestingly, they found restricting P27^{Kip1} levels by using gene deficient T-cells made the cells more susceptible to apoptosis, but inhibited their ability to arrest prior to death. The data suggest a very close link between P27^{Kip1}'s role in proliferation and apoptosis in these cells. While its up-regulation appears to directly induce apoptosis, cytokine deprivation may not require P27^{Kip1} to induce apoptosis, but rather activates a phosphorylation-dependent death program (Janicke et al., 1996).

The camptothecin experiment also showed that phosphatidylserine externalization correlated temporally with increased $P27^{Kip1}$ protein steady state levels after 6 hours of exposure. The evidence provided by the IL-2 deprivation and camptothecin experiments suggests that $P27^{Kip1}$ is an integral initiator of the apoptotic response in mouse HT-2 cells. Both inducers inhibit mechanisms in early stages of the cell cycle, providing a reasonable explanation for the up-regulation of $P27^{Kip1}$ at the G1/S phase checkpoint. A build up of cells in G1 resulting from cytokine withdrawal would promote $P27^{Kip1}$ activity to move cells out of the cycle by initiating apoptosis. Accumulation in S phase could slow the progression of cells from G1 to S, contributing to the hyperactivity of the apoptotic inhibitor. The third inducer, however, initiated a contrary response in $P27^{Kip1}$ regulation, as steady state levels decreased at 24 hours post-induction. Because staurosporine induced cell cycle arrest in G2/M phase prior to fragmentation, it blocked cells from dividing and reentering the initial growth phase. Cells beginning in S or G2/M phase for IL-2 deprivation and G2/M phase for camptothecin experiments could divide and reenter G1, increasing demand for $P27^{Kip1}$ activity and stimulating inhibitor production. In future experiments, we propose to quantify $P27^{Kip1}$ via chemiluminescence detection, to determine steady-state levels in IL-2 deprived cells, in which all cells reach the G1/S checkpoint prior to apoptosis. High levels of $P27^{Kip1}$ will also likely be observed in camptothecin exposed cells, where all cells except those beginning the treatment in S-phase will pass through this checkpoint. Finally, staurosporine-treated cells will likely have diminished $P27^{Kip1}$ levels, as only those cells beginning in G1 will pass the checkpoint.

Future Work

This study aimed to better understand the mechanisms that control programmed cell death in T-lymphocytes. We have identified appropriate cell and inducer concentrations to initiate apoptosis in this growth factor-dependent cell line. Early and late stage morphological changes have been identified in a time course fashion, and evidence presented in this study suggests that the mode of induction dictates cell cycle distribution and arrest prior to apoptosis. This body of work will serve as the primary foundation as we continue to investigate apoptosis regulation in HT2 cells.

In addition to carrying out chemiluminescence detection in future work, we also plan to improve documentation of the time course associated with programmed cell death by quantifying late-stage apoptosis by flow cytometry using TUNEL assays. Finally, using siRNA-or morpholino-mediated gene silencing, we hope to functionally characterize the role of $P27^{Kip1}$ during apoptosis in HT-2 cells. By inhibiting the production of RNA transcripts and/or protein synthesis, we aim to determine if $P27^{Kip1}$ promotes or discourages apoptosis, and how the inducer influences this inhibitor's function.

As our research continues, we also plan to explore the reversibility of the apoptotic response with these specific inducers. Previous unpublished studies have evaluated the reversibility of apoptosis with IL-2 withdrawal, and found that T-cells were able to re-enter the cell cycle, regain function and viability with the reintroduction of the cytokine 24 hours after deprivation (Lauzon, unpublished observations). Extensive work has been performed on cancer cells and their ability to regain function following transient apoptosis (Tang et al., 2009). These studies have found that even late state-apoptotic

cancer cells in several cell lines were able to recover, although some with permanent genetic alterations (Tang et al., 2012). We hope to investigate whether apoptosis induced in HT-2 T-lymphocytes with camptothecin or staurosporine is also reversible, and if so, what is the time course of reversibility. Furthermore, we would like to address if the reversibility of apoptosis-mediated cell cycle arrest is phase-dependent.. Reversibility of apoptosis may contribute to our understanding of failed cancer treatments or recurrent cancers.

Acknowledgments

I would first like to thank the Union College Department of Biological Sciences for providing laboratory space and instrument access. Additionally, this project would not have been possible without the financial support from the Union College Student Research Grants. Finally, I would like to offer special thanks to my thesis advisor, Robert J. Lauzon, PhD, for his thoughtful guidance, enthusiastic teaching, and immeasurable patience throughout the evolution of this research. It has been an absolute pleasure working with him.

References

Albert, M., Sauter, B., & Bhardwaj, N. (1998). "Dendritic cells acquire antigen from apoptotic cells and induce class-I restricted CTLs," *Nature* (392) 86–89.

Bertrand, T., Solary, E., O'Connor P., Kohn, K., & Pommier Y. (1994). "Induction of a common pathway of apoptosis by staurosporine," *Exp. Cell Res.* (211) 314-321.

Bell, B., Leverrier, S., Weist, B., Newton, R., Arechiga, A., Luhrs, K. Morrissette, N., & Walsh, C. (2008) "FADD and caspase-8 control the outcome of autophagic signaling in proliferating T cells*," Proc. Natl. Acad. Sci. U.S.A.,* (43) 16409 16410.

Bell, B., & Walsh, C. (2009). "Coordinate regulation of autophagy and apoptosis in T cells by death effectors: FADD or foundation," *Autophagy*, (5) 238-240.

Belmokhtar, C., Hillion, J., & Seagal-Bendirdjian, E. (2001). "Staurosporine induces apoptosis through both caspase-dependent and caspase-independent mechanisms." *Nature,* (20) 3354-3362.

Blagosklonny, M. (2011). "Cell cycle arrest is not senescence," *Aging,* (3) 94-101.

Bruggeman, F., Novak, B., Conradi, R., Csikasz-Nagy, A., Snoep, J., Ciliberto, A., & Westernhoff, H. (2010). "Restriction point control of the mammalian cell cycle via the cyclin E/Cdk2:p27 complex," *FEBS,* (227) 357-367.

Castro, A., Lemos C., Falcao, A., Fernandes, A., Glass, N., & Videira, A. (2010). "Rotenone enhances the antifungal properties of staurosporine," *Eukaryotic Cell,* (9) 906-914.

Crispin, J., Apostolidis, S., Finnell, M., & Tsokos, G. (2011). "Induction of PP2A B beta, a regulator of IL-2 deprivation-induced T-cell apoptosis, is deficient in systemic lupus erythematosus," *Natl. Acad. Sci.,* (108) 12443-12448.

Ch'en, I., Beisner, D., Degterev, A., Lynch, C., Yuan, J., Hoffmann, A., & Hedrick S. (2008)."Antigen-mediated T-cell expansion regulated by parallel pathways of death," *Proc. Natl. Acad. Sci. U.S.A.,* (45) 17463-17468.

Drexler, H. & Pebler, S. (2003). "Inducible $p27^{Kip1}$ expression inhibits proliferation of K562 cells and protects against apoptosis induction by proteasome inhibitors," *Cell Death and Diff.,* (10) 290-301.

Elmore, S. (2007). "Apoptosis: a review of programmed cell death," *Toxicol Pathol*, (4): 495 -516.

Eymin, B. & Brambilla, E. (2004). "The yin and the yang of p27Kip1 as a target for cancer therapy," *Eur. Respir.,* (23) 663-664.

Fan, L., Yalin, M., Liu, Y., Zheng, D., & Huang, G. (2014). "Silymarian induces cell cycle arrest and apoptosis in ovarian cancer cells," *Euro. J. Pharm.,* (743) 79-88.

Fulda, S. & Debatin, K (2006). "Extrinsic vs. intrinsic apoptosis pathways in anticancer chemotherapy," *Oncogene*, (25) 4798-4811.

Hanahan D. & Weinberg R. (2000). "The hallmarks of cancer," *Cell* (100) 57-70.

Hertzberg, R., Caranfa, M., & Hecht, S. (1989). "On the mechanism of topoisomerase I inhibition by camptothecin: Evidence for binding to an enzyme-DNA complex," *Biochemistry*, (28) 4629-4638.

Hiromura, K., Pippin, J., Fero, M., Roberts, J., & Shankland, S. (1999). "Modulation of apoptosis by the cyclin-dependent kinase inhibitor $p27^{kip1}$," (103) 597-604.

Huleatt, J., Cresswell, J., Bottomly, K., & Crispe, N. (2003). "$P27^{kip1}$ regulates the cell cycle arrest and survival of activated T lymphocytes in response to interleukin-2 withdrawal," *Immunology,* (108) 493-501.

Ishii, T, Fujishiro, M., Masuda, M., (2004) "Effects of p27Kip1 on cell cycle status and viability in A549 lung adenocarcinoma cells," *Eur. Resp. J.,* (23) 665-670.

Jacobs, S., Basak, S., Murray, J., Pathak, N., & Attardi, L. (2007). "Siva is an apoptosis selective p53 target gene important for neuronal cell death," *Cell Death and Diff.,* (14) 1374-1385.

Jain, M., Sowmya K., Samar K., & Desai A. (2014). "An Insight to Apoptosis," *Journal of Research and Practice in Dentistry,* 2014 (1) 1-12.

Janicke, R., Walker, P., Lin X., &Porter, A. (1996). "Specific cleavage of the retinoblastomaprotein by an ICE-like protease in apoptosis," *EMBO J.,* (15) 6969-6978.

Keebler, J. & Gilmore, A. (2007). "Apoptosis commitment – translating survival signals into decisions on mitochondria," *Nature*, (17) 976-984.

Kerr, J., Wyllie A., & Currie A. (1972). "Apoptosis" a basic biological phenomenon with wide ranging implications on tissue kinetics," *Br. J. Cancer,* (4) 239-57.

Kroemer, G. (2014). "Regulated necrosis," *Seminars in Cell and Dev Bio* (35) 1.

Kurosaka, K., Takahashi, M., Watanabe, N., & Kobayashi, Y. "Silent cleanup of very early apoptotic cells by macrophages," *J Immunol*, (9) 4672-4679.

Kyle, A., Gandolfo, M., Baker, J., & Minchinton, A. (2014). "Camptothecins: Tissue penetration and implications for therapy," *Cancer Res,* (74) 827.

Levkau, B., Koyama, H., Raines, E., Clurman, B., Herren, B., Orth, K., Roberts, J., & Ross, R. (1998). Cleavage of $p21^{CipqWaf1}$ and $p27^{Kip1}$ mediates apoptosis in endothelial cells through activation of the Cdk2: role of a caspase cascade," *Molec. Cell*, (1) 553-563.

Li, Q., Sato, E., Zhu, X., & Inoue, M. (2009). "A simultaneous release of SOD1 with cytochrome c regulates mitochondria-dependent apoptosis," *Mol. Cell Biochem,* (322) 151-159.

Lian, J., Zubovitz, J., Petrocelli, T., Kotchetkov, R., Connor, K., Han, K., Lee, J., Ciarallo, J., Catzavelos, C., Beniston, R., Franssen, E., & Slingerland, J. (2002) "PKB/Akt phosphorylates p27, impairs nuclear import of p27 and opposes p27 mediated G1 arrest," *Nature Med*, (8) 1153–1160.

Masuda, A., Osada, H., Yatabe, Y., Kozaki, K., Tatematsu, Y., Takahashi, T., Hida, T., Takahashi, T., & Takahashi, T. (2001). "Protective function of $p27^{KIP1}$ against apoptosis in small cell lung cancer cells in unfavorable microenvironments," *Am. J. Path.,* (158) 87-96.

Mercier, S., Diepenbroek, B., Martens, D, Wijffels, R., & Streefland, M. (2013). "Cell cycle and apoptosis in PER.C6 cultures," *BMC Proceedings,* (7) 48.

McKenzie, M., Liolitsa, D., & Hanna, M. (2004). "Mitochondrial disease: mutations and mechanisms," *Neurochem Res* (29) 589-600.

Pommier Y. (2006). "Topoisomerase I inhibitors: Camptothecins and beyond," *Nat. Rev. Cancer,* 789-802.

Prasad, K., & Prabhakar, B. (2003). "Apoptosis and autoimmune disorders," *Autoimmunity,* (36) 323-330.

Prunell, G., Arboleda, V., & Troy C. (2005). "Caspase function in neuronal death: delineation of the role of caspases in ischemia." *Curr Drug Targets CNS Neurol Disord* (4) 51-61.

Rohn, T., Head, E., Nesse, W., Cotman, C., Cribbs, D. (2001). "Activation of caspase-8 in the Alzheimer's disease brain," *Neurobiol Dis* (8) 1006-1016.

Savill, J., Dransfield, I., Gregory, C., & Haslett, C. (2002). A blast from the past: clearance of apoptotic cells regulates immune responses." *Nature,* (2) 965-975

Savill, J., Fadok V. (2000). Corpse clearance defines the meaning of cell death. *Nature*, (407) 784-788.

Schleich, K. & Lavrik, I. (2013). Systems Biology of Apoptosis, *Springer New York,* pp. 33-56.

Simenc, J. & Lipnik-Stangeli, M. (2012). "Staurosporine induces apoptosis and necroptosis in cultured rat astrocytes," *Drug and Chem. Tox.,* (35) 399-405.

Tang, HL., Tang, HM., Mak, K., Hu, S., Wang, S., Wong, K., Wong, C., Wu, H., Law, H., Liu, K., Talbot, C., Lau, W., Montell, D., & Fung, M. (2012). "Cell survival, DNA damage, and oncogenic transformation after a transient and reversible apoptotic response," *Molec. Bio. Cell,* (23) 2240-2252.

Tang, H., Yuen, K., Tang, H., & Fung, M. (2009). "Reversibility of apoptosis in cancer cells," *Brit. J. Cancer* (100) 118-122.

Tong, Z., Yan, H., Liu, W. (2014). Interleukin-17F attenuates H202-induced cell cycle arrest," *Cell. Immunol.,* (278) 74-77.

Tsai, T., Chuang, Y., Lin, Y., Wan, S., Chen, C., & Lin, C. (2013). "An emerging role for the antiinflammatory cytokine interleukin-10 in dengue virus infection," *Biomed. Sci.,* (20) 40-49.

Vaux, D. (1993). "Toward an understanding of the molecular mechanisms of physiological cell death." *Proc. Natl. Acad. Sci*. (90) 786–789.

Voll, R., Herrmann, M., Roth, E., Stach, C. & Kalden, J. (1997). "Immunosuppressive effects of apoptotic cells," *Nature,* (390) 350–351.

Walsh, C. (2014). "Grand challenges in cell death and survival: apoptosis vs. necroptosis," *Frontiers in Cell and Developmental Biology,* 2 (3) 1-4

Zare-Mirakabadi, A., Sarzaeem, A., Moradhaseli, S., Sayad, A., & Negahdary, M. (2012)."Necrotic effect versus apoptotic nature of camptothecin in human cervical cancer cells," *Iran J. Cancer Prev,* (3) 109-116.

Zeng, C., Zhang, X., Lin, K., Ye, H., Feng, S., Zhang, H., & Chen, Y. (2012). "Camptothecin induces apoptosis in cancer cells via microRNA-125b-mediated mitochondrial pathways," *Amer. Soc. Pharm. Exp. Ther.,* (81) 578-586.

Zong, Z., Fujikawa-Yamamoto, K., Li, A., Yamaguchi, N., Chang Y., Murakami, M., Odashima, S., & Ishikawa, Y. (1999). "Both low and high concentrations of staurosporine induce G1 arrest through down-regulation of cyclin E and cdk2 expression," *Cell Structure Function*, (6) 457-463.

Appendix

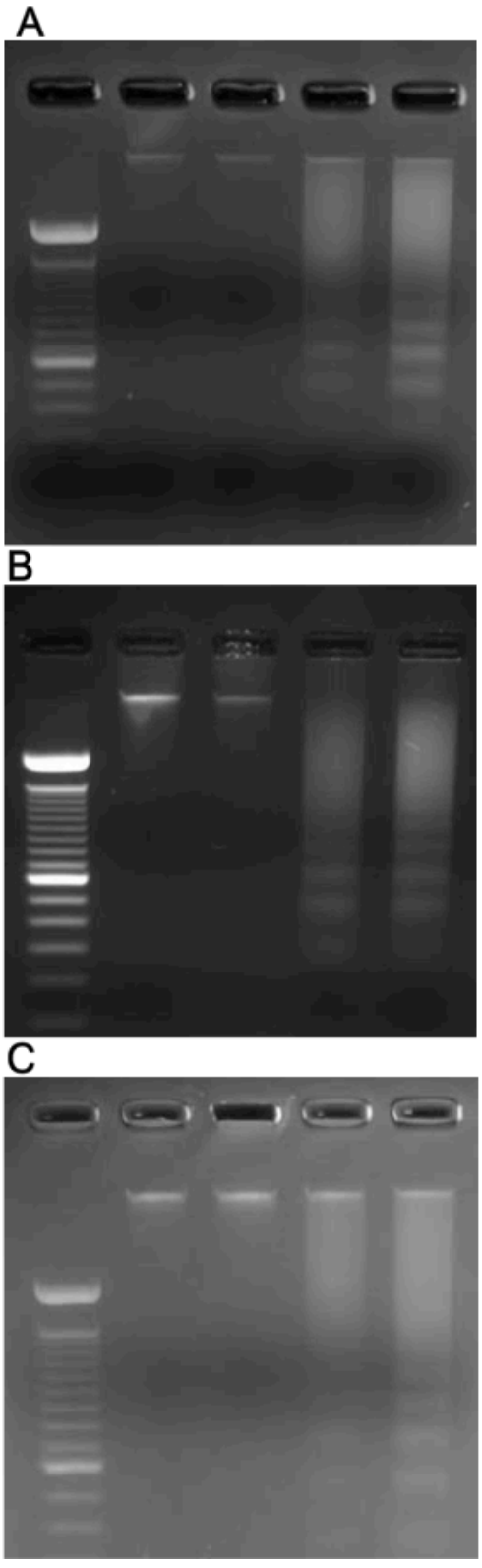

Figure 1. Electrophoresis gel DNA fragmentation after 24-hour incubation. The gels were used to determine optimal cell and/or toxin concentrations for each apoptosis inducer. A) IL-2 deprivation experiment, lanes 1-5 (from left to right): MW markers, IL-2(+) 100,000 cells/mL, IL-2(+) 200,000 cells/mL, IL-2(-) 100,000 cells/mL, IL-2(-) 200,000 cells/mL. B) Camptothecin (6mM) experiment, lanes 1-5 (from left to right): MW markers, Campto(-) 100,000 cells/mL, Campto(-) 200,000 cells/mL, Campto(+) 100,000 cells/mL, Campto(+) 200,000 cells/mL C) Staurosporine (1uM) experiment, lanes 1-5 (from left to right): MW markers, Stauro(-) 100,000 cells/mL, Stauro(-) 200,000 cells/mL, Stauro(+) 100,000 cells/mL**,** Stauro(+) 200,000 cells/mL. The optimal cell concentration for all experiments was found to be 200,000 cells/mL. A camptothecin concentration of 6 mM was sufficient to demonstrate apoptotic DNA laddering, while staurosporine induced laddering at a concentration of 1uM.

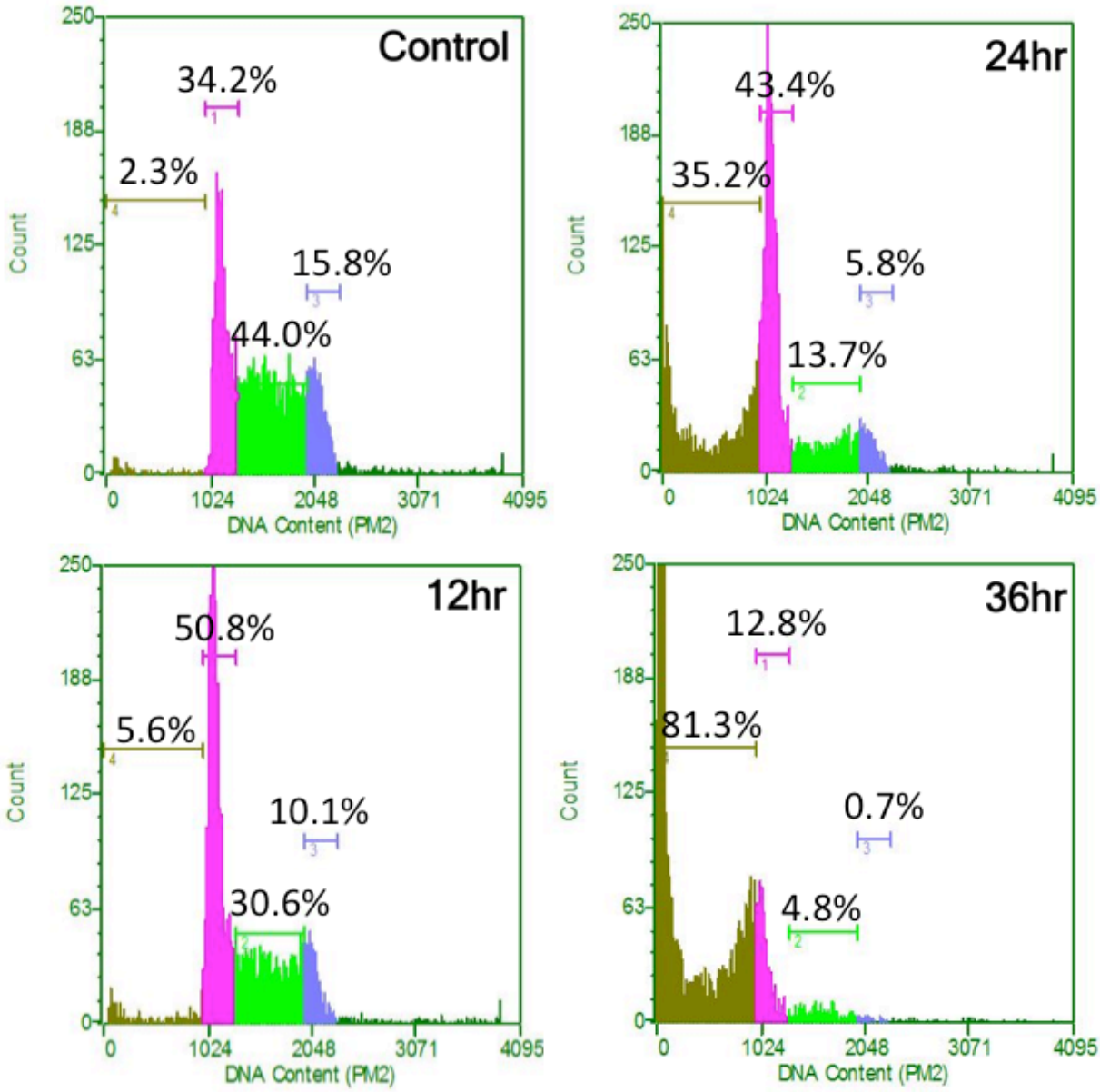
Control
34.2%
2.3%
15.8%
44.0%
24hr
43.4%
35.2%
5.8%
13.7%
12hr
50.8%
5.6%
10.1%
30.6%
36hr
12.8%
81.3%
0.7%
4.8%
Count
DNA Content (PM2)
0
63
125
188
250
1024
2048
3071
4095

Figure 2. Flow cytometry cell cycle analysis following a 36-hour time course IL-2 deprivation treatment. HT-2 cells were incubated with 7-aminoactinomycin D (7-AAD) to determine changes in cell cycle distribution following apoptosis induction following IL-2 deprivation. Control HT-2 cells grown in IL-2 (+) media demonstrate typical cell cycle distribution patterning with brown representing sub-G1 DNA content, pink representing cells with G1 DNA content, green representing cells in S phase, and blue representing cells in G2/Mitosis. Cells begin to accumulate in G1 at 12 hours following IL-2 deprivation, and subsequently begin to fragment (sub-G1 peak) at 24 hours. By 36 hours, the majority of cells have died. Percent values for each phase of the cell cycle (DNA content) are indicated in each histogram.

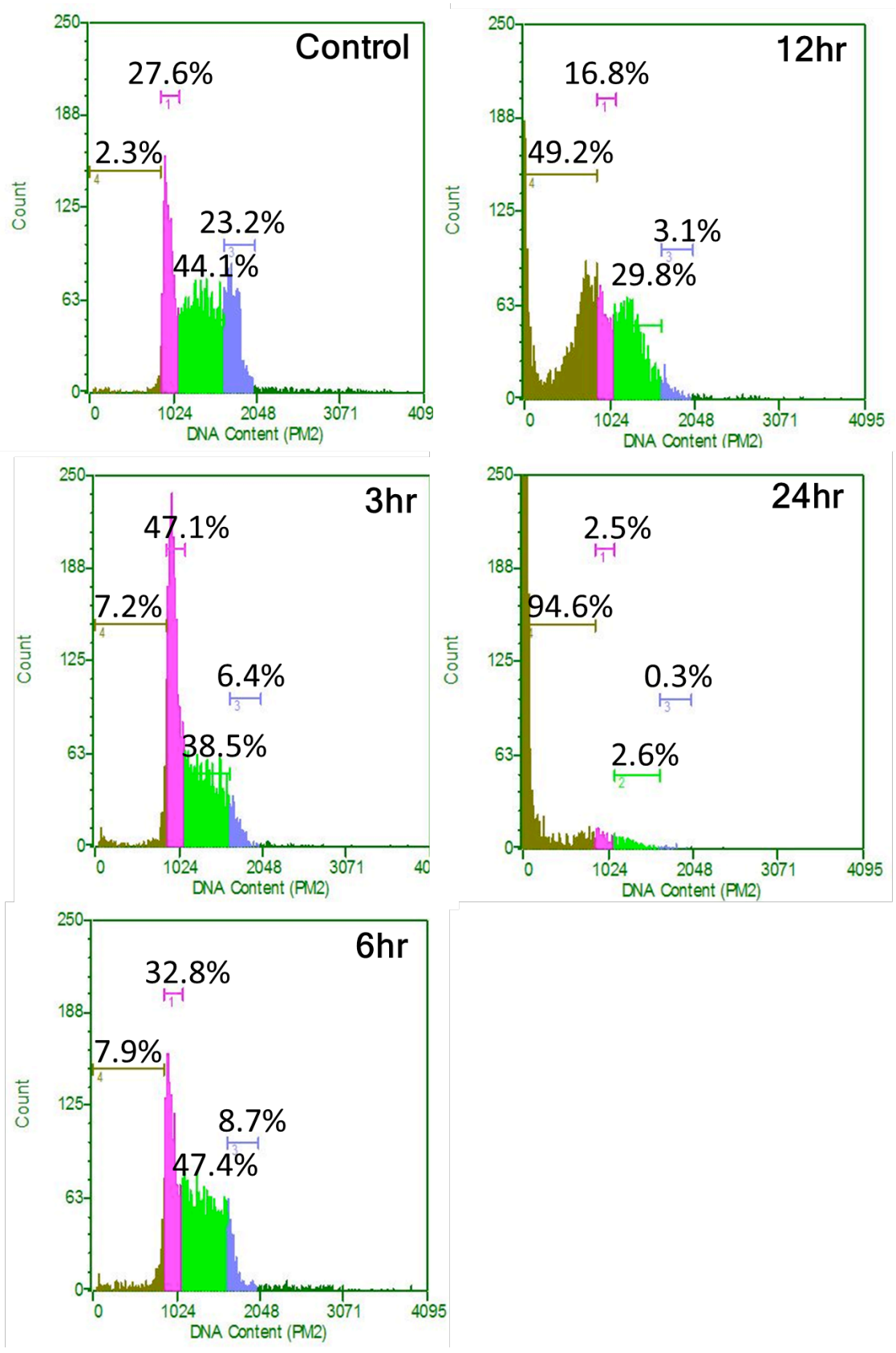
Control
27.6%
2.3%
23.2%
44.1%
12hr
16.8%
49.2%
3.1%
29.8%
3hr
47.1%
7.2%
6.4%
38.5%
24hr
2.5%
94.6%
0.3%
2.6%
6hr
32.8%
7.9%
8.7%
47.4%
Count
DNA Content (PM2)
0
1024
2048
3071
4095
63
125
188
250

Figure 3. Flow cytometry cell cycle analysis following a 24-hour time course with 6 mM camptothecin treatment. HT-2 cells were incubated with 7-aminoactinomycin D (7-AAD) to determine changes in cell cycle distribution following apoptosis induction with camptothecin. Control cells grown in IL-2 (+) media demonstrate typical cell cycle distribution patterning with brown representing sub-G1 DNA content, pink representing cells with G1 DNA content, green representing cells in S phase, and blue representing cells in G2/Mitosis. Initial accumulation of cells in G1-phase occurs at 3 hours following camptothecin exposure and the majority of cells accumulate in S-phase by 6 hours of incubation. Notable death is observed after 12 hours of exposure (sub-G1 DNA peak) and nearly all cells have died at 24 hours**.**

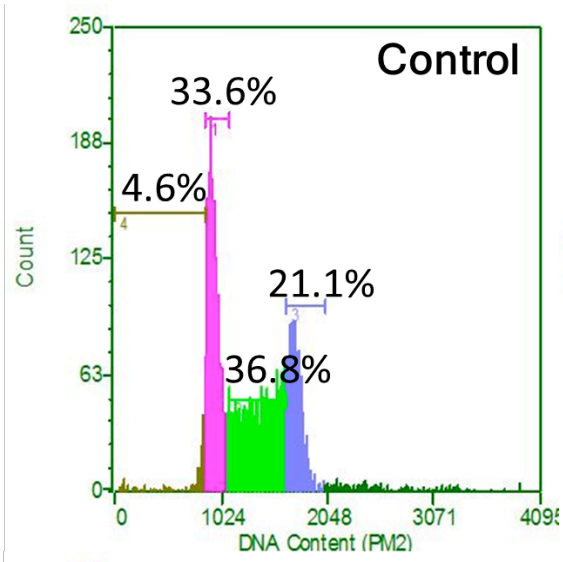
Control
33.6%
4.6%
21.1%
36.8%
Count
DNA Content (PM2)

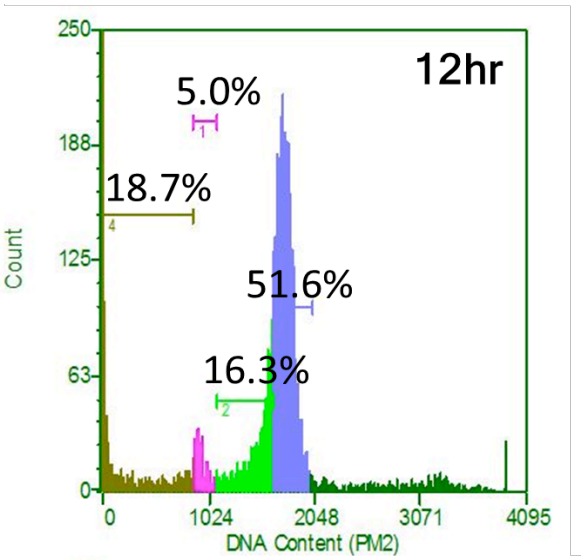
12hr
5.0%
18.7%
51.6%
16.3%
Count
DNA Content (PM2)

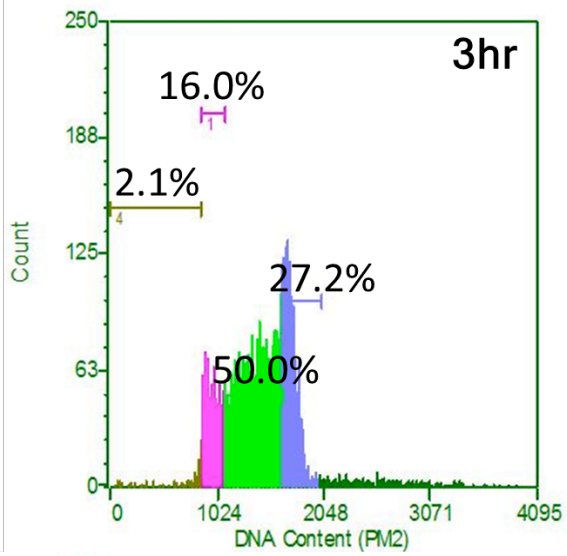
3hr
16.0%
2.1%
27.2%
50.0%
Count
DNA Content (PM2)

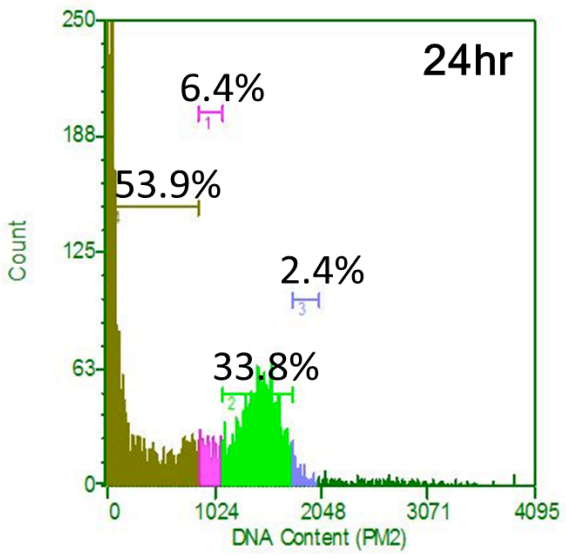
24hr
6.4%
53.9%
2.4%
33.8%
Count
DNA Content (PM2)

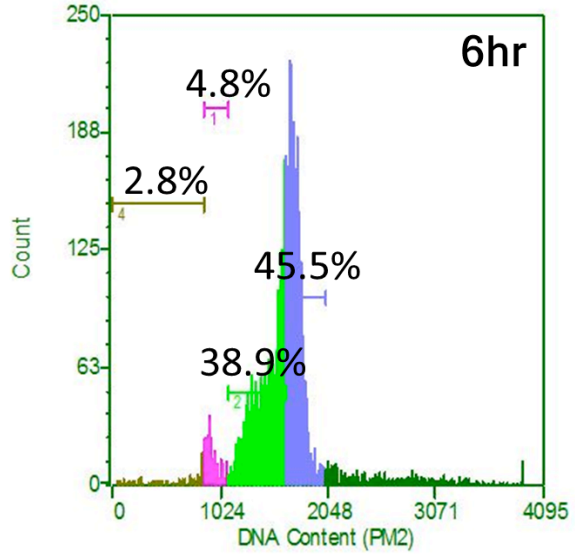
6hr
4.8%
2.8%
45.5%
38.9%
Count
DNA Content (PM2)

Figure 4. Flow cytometry cell cycle analysis following a 24-hour time course with 1 uM staurosporine treatment. HT-2 cells were incubated with 7-aminoactinomycin D (7-AAD) to determine changes in cell cycle distribution following apoptosis induction with staurosporine. Control cells grown in IL-2 (+) media demonstrate a typical cell cycle distribution pattern with brown representing cells with sub-G1 DNA content, pink representing cells with G1 DNA content, green representing cells in S phase, and blue representing cells in G2/Mitosis. Accumulation of cells in S and G2/M phases of the cell cycle occurs 3 hours following staurosporine exposure. This accumulation shifts toward the G2/M phase after 6 hours, and most cells have accumulated in G2/M phase by 12 hours. By 24 hours, the majority of cells have died.

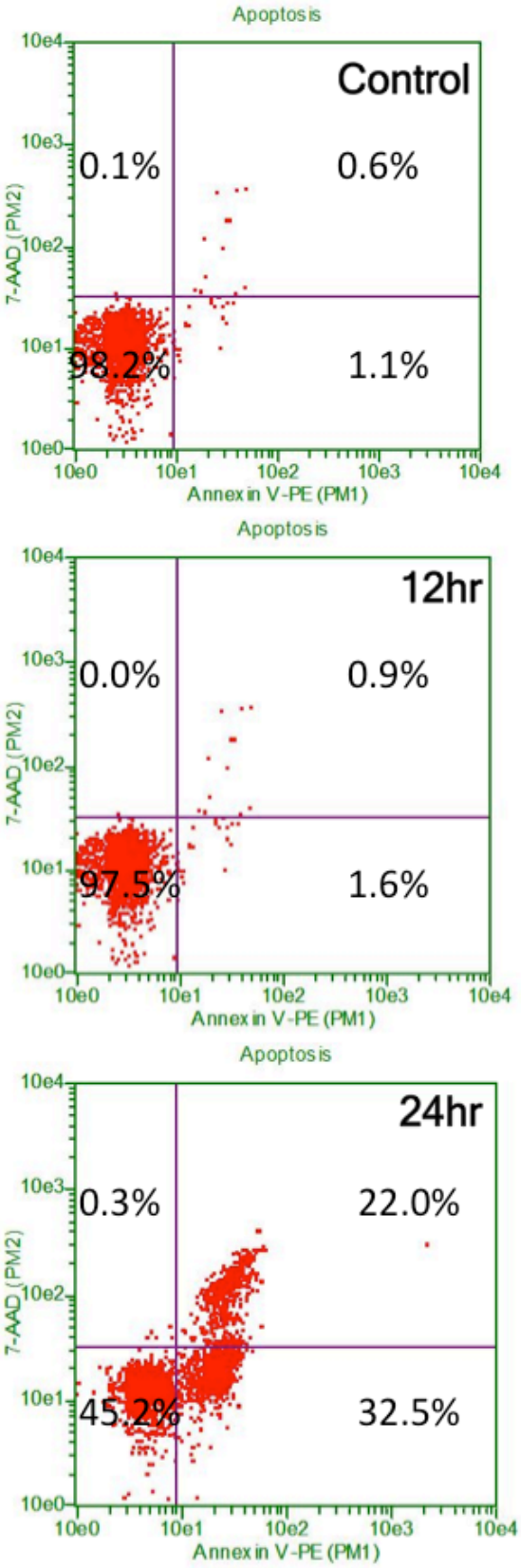
Apoptosis
Control
0.1%
0.6%
98.2%
1.1%
7-AAD (PM2)
Annexin V-PE (PM1)
10e0
10e1
10e2
10e3
10e4
Apoptosis
12hr
0.0%
0.9%
97.5%
1.6%
7-AAD (PM2)
Annexin V-PE (PM1)
Apoptosis
24hr
0.3%
22.0%
45.2%
32.5%
7-AAD (PM2)
Annexin V-PE (PM1)

Figure 5. Flow cytometry analysis of Annexin V staining following a 24 hour IL-2 deprivation time course. Since phosphatidylserine externalization is an early event during apoptosis, Annexin V staining was used to identify the time required to initiate apoptosis following deprivation. Healthy, non-apoptotic cells are shown in the lower left-hand quadrant (7-AAD and Annexin V-PE negative). Early stage apoptosis marked by phosphatidylserine externalization and Annexin V binding is observed in the lower right-hand quadrant (7-AAD negative, annexin V positive). Late stage apoptosis marked by plasma membrane degradation and 7-AAD staining is observed in the upper right-hand quadrant (7-AAD and annexin V positive). Early stages of apoptosis in IL-2 deprived cells are observed to occur between 12 and 24 hours following IL-2 deprivation.

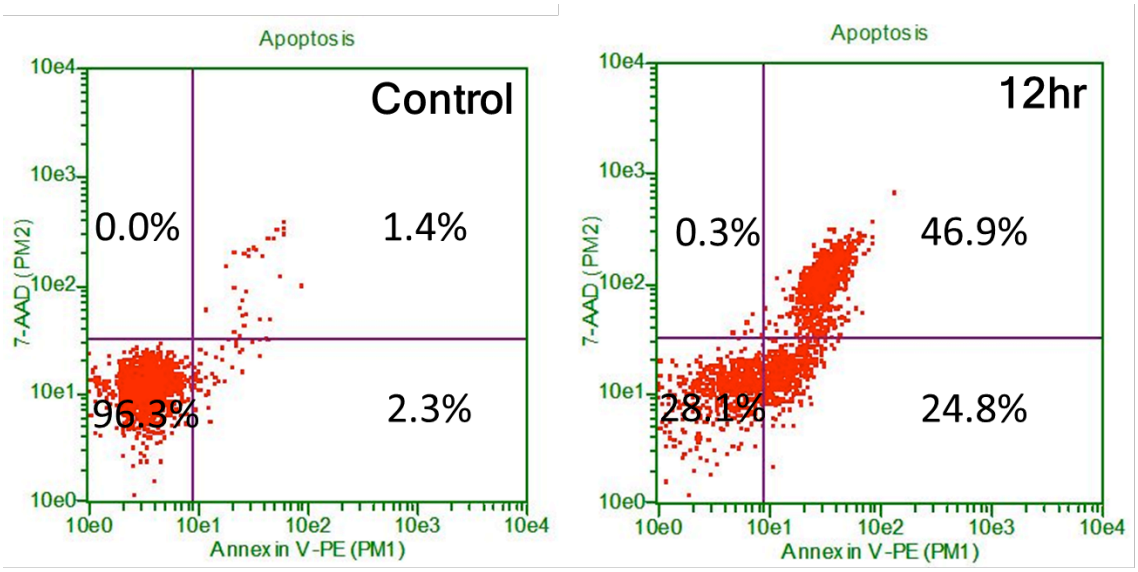
Apoptosis
Control
0.0%
1.4%
96.3%
2.3%
7-AAD (PM2)
Annexin V-PE (PM1)
10e0
10e1
10e2
10e3
10e4

Apoptosis
12hr
0.3%
46.9%
28.1%
24.8%
7-AAD (PM2)
Annexin V-PE (PM1)
10e0
10e1
10e2
10e3
10e4

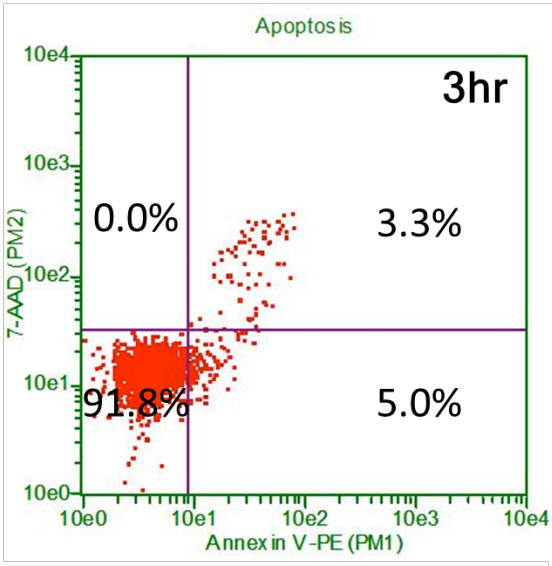
Apoptosis
3hr
0.0%
3.3%
91.8%
5.0%
7-AAD (PM2)
Annexin V-PE (PM1)
10e0
10e1
10e2
10e3
10e4

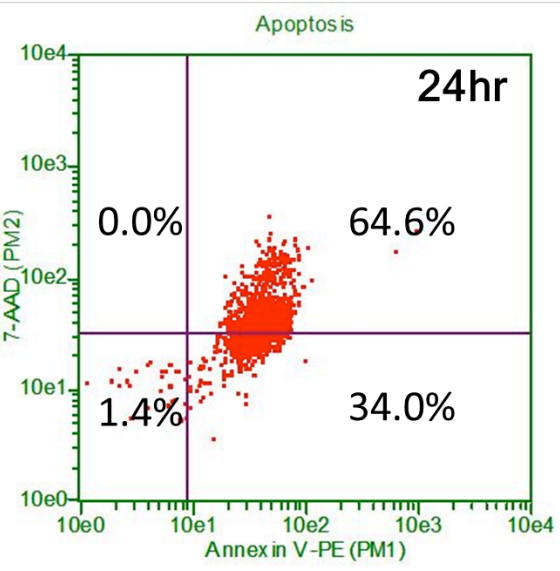
Apoptosis
24hr
0.0%
64.6%
1.4%
34.0%
7-AAD (PM2)
Annexin V-PE (PM1)
10e0
10e1
10e2
10e3
10e4

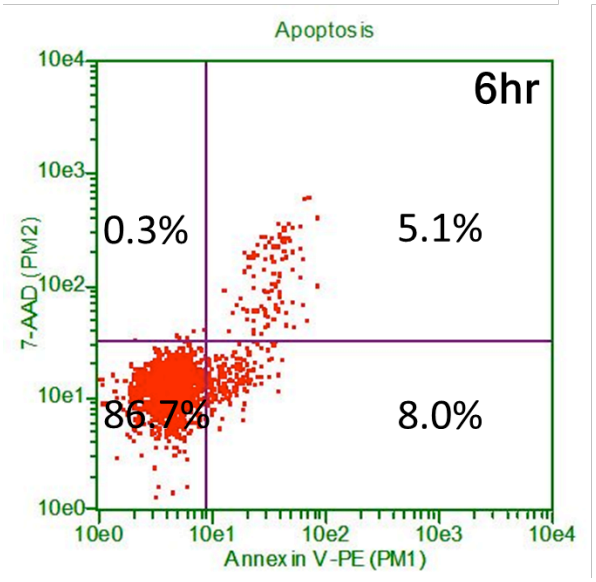
Apoptosis
6hr
0.3%
5.1%
86.7%
8.0%
7-AAD (PM2)
Annexin V-PE (PM1)
10e0
10e1
10e2
10e3
10e4

Figure 6. Flow cytometry analysis of Annexin V staining following a 24-hour time course with 6 mM camptothecin. Since phosphatidylserine externalization is an early event during apoptosis, Annexin V staining was used to identify the time required to initiate apoptosis following induction with camptothecin. Healthy, non-apoptotic cells are shown in the lower left-hand quadrant (7-AAD and Annexin V-PE negative). Early stage apoptosis marked by phosphatidylserine externalization and Annexin binding is observed in the lower right-hand quadrant (7-AAD negative, annexin V positive). Late stage apoptosis marked by plasma membrane degradation and 7-AAD staining is observed in the upper right-hand quadrant (7-AAD and annexin V positive). Significant induction of apoptosis commences after 3 hours of incubation, and the majority of cells enter late stages of apoptosis by 12 hours.

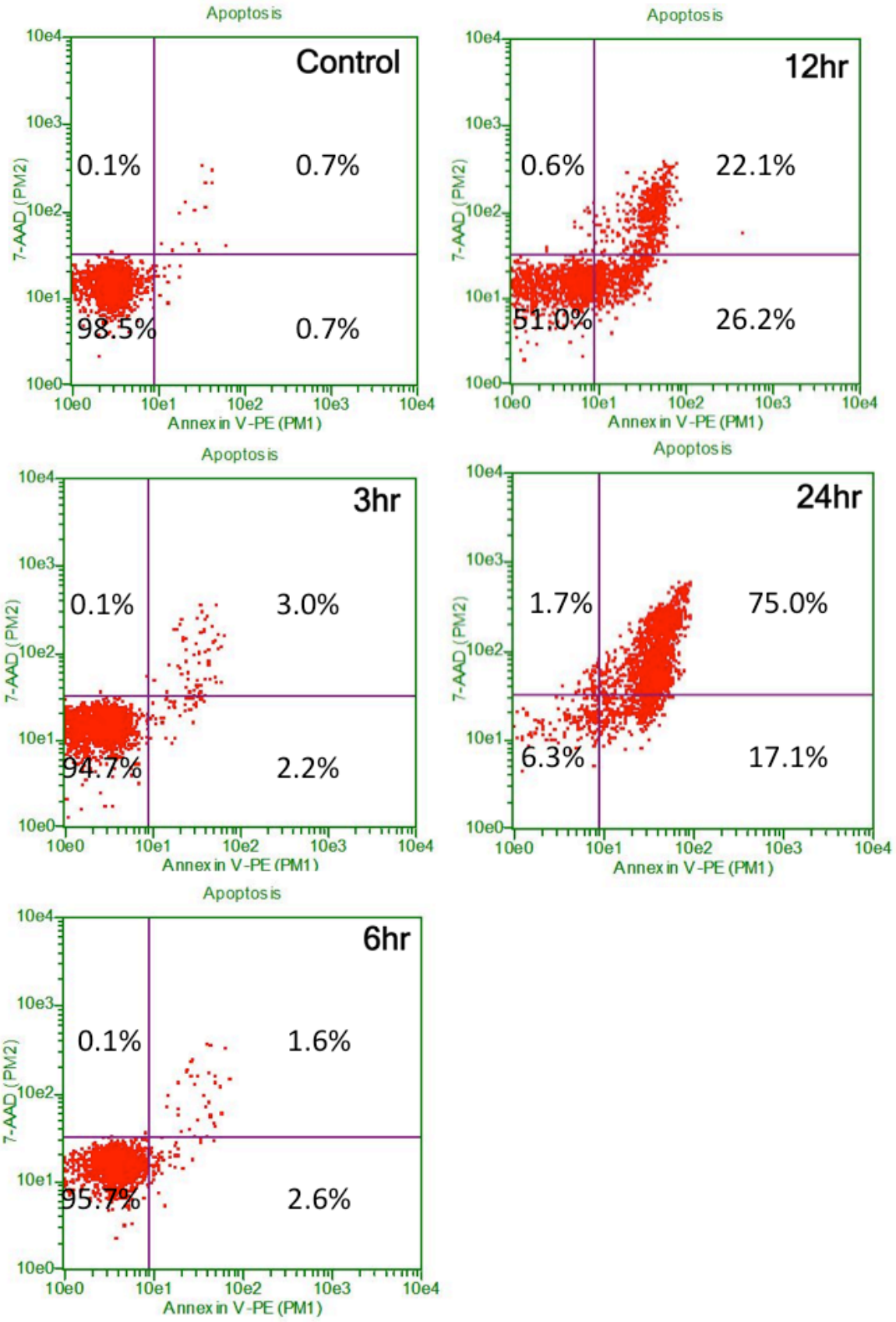
Apoptosis
Control
0.1%
0.7%
98.5%
0.7%
7-AAD (PM2)
Annexin V-PE (PM1)
Apoptosis
12hr
0.6%
22.1%
51.0%
26.2%
7-AAD (PM2)
Annexin V-PE (PM1)
Apoptosis
3hr
0.1%
3.0%
94.7%
2.2%
7-AAD (PM2)
Annexin V-PE (PM1)
Apoptosis
24hr
1.7%
75.0%
6.3%
17.1%
7-AAD (PM2)
Annexin V-PE (PM1)
Apoptosis
6hr
0.1%
1.6%
95.7%
2.6%
7-AAD (PM2)
Annexin V-PE (PM1)

Figure 7. Flow cytometry analysis of Annexin V staining following a 24-hour time course with 1 uM staurosporine. Since phosphatidylserine externalization is an early event during apoptosis, Annexin V staining was used to identify the time required to initiate apoptosis following induction with camptothecin. Healthy, non-apoptotic cells are shown in the lower left-hand quadrant (7-AAD and Annexin V-PE negative). Early stage apoptosis marked by phosphatidylserine externalization and Annexin V binding is observed in the lower right-hand quadrant (7-AAD negative, annexin V positive). Late stage apoptosis marked by plasma membrane degradation and 7-AAD staining is observed in the upper right-hand quadrant (7-AAD and annexin V positive). Early apoptosis is observed between 6 and 12 hours of incubation and the majority of cells have entered late-stage apoptosis by 24 hours.

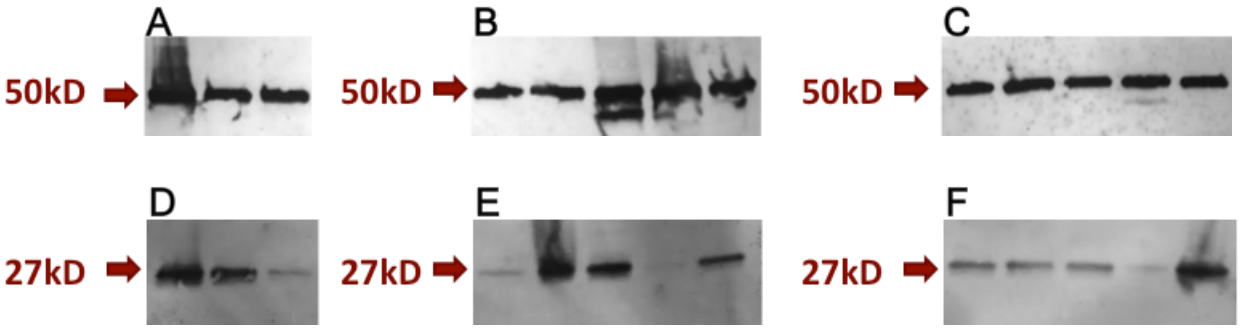
A
B
C
50kD
50kD
50kD
D
E
F
27kD
27kD
27kD

Figure 8. SDS-PAGE and immunoblotting with anti-tubulin and $P27^{Kip1}$ specific antibodies. Alpha-tubulin was used as a housekeeping control. A) IL-2 deprivation with anti-tubulin staining: lanes 1-3 (from left to right) depict 12hr IL-2(-), 24hr IL-2(-), 24hr IL-2(+). B) 6 mM camptothecin with anti-tubulin staining: lanes 1-5 (from left to right) depict 3hr Campto(+), 6hr Campto(+), 12hr Campto(+), 24hr Campto(+), 24hr Campto(-). C) 1 μM staurosporine with anti-tubulin staining: lanes 1-5 (from left to right) depict 3hr Stauro(+), 6hr Stauro(+), 12hr Stauro(+), 24hr Stauro(+), 24hr Stauro(-). D) IL-2 deprivation with anti-$P27^{Kip1}$ staining: lanes 1-3 (from left to right) depict 12hr IL-2(-), 24hr IL-2(-), 24hr IL-2(+). E) 6 mM Camptothecin with anti-$P27^{Kip1}$ staining: lanes 1-5 (from left to right) depict 3hr Campto(+), 6hr Campto(+), 12hr Campto(+), 24hr Campto(+), 24hr Campto(-). F) 1 μM staurosporine with anti-$P27^{Kip1}$ staining: lanes 1-5 (from left to right) depict 3hr Stauro(+), 6hr Stauro(+), 12hr Stauro(+), 24hr Stauro(+), 24hr Stauro(-). $P27^{Kip1}$ protein steady state levels increase within 12 and 6 hours following IL-2 and camptothecin treatments, respectively.